THE PMTRAS ROLL ASPECT SYSTEM ON RHESSI

G. J. HURFORD and D. W. CURTIS
Space Sciences Laboratory, University of California, Berkeley, CA 94720-7450, U.S.A.
(e-mail: ghurford@ssl.berkeley.edu)

(Received 17 August 2002; accepted 17 August 2002)

Abstract. High-resolution solar hard X-ray imaging on the Reuven Ramaty High-Energy Solar Spectroscopic Imager (RHESSI) spacecraft is achieved by a set of rotating modulation collimators. The interpretation of the observed time-modulated X-ray flux in terms of high-resolution, accurately located images requires continuous, arc-minute roll aspect, which at present is provided by the 'Photo-Multiplier Tube Roll Aspect System' (PMTRAS). This paper describes the PMTRAS operating principles, hardware implementation, calibration, performance and data analysis approach, with emphasis on its effect on RHESSI imaging.

1. Introduction

The Reuven Ramaty High-Energy Solar Spectroscopic Imager (RHESSI) is a NASA Small Explorer (SMEX) mission to study the acceleration and transport of high-energy particles in solar flares (Lin *et al.*, 2002). Observationally this is accomplished by high-resolution imaging spectroscopy of X-rays and gamma-rays from 3 keV through 17 MeV with angular resolution as high as 2.3 arc sec. Achieving high angular resolution in this energy range requires indirect imaging techniques. In this case a set of 9 modulation collimators are mounted on a rotating spacecraft. Each collimator consists of a pair of widely spaced grids that alternately transmits and blocks part of the incident X-ray flux as the spacecraft rotates. The imaging information is encoded in the time-modulated lightcurves (Hurford *et al.*, 2002). The data consist primarily of time- and energy-tagged photons from which the image is subsequently reconstructed by ground-based analysis software (Schwartz *et al.*, 2002).

The RHESSI spacecraft rotates at a nominal 15 rpm about an axis directed at the Sun. One of the enabling features of this imaging approach is that spacecraft pointing requirements (0.2 deg) are based on the 1-degree imager field of view, instead of the 2.3-arc sec angular resolution. A high-bandwidth subarc-second pitch and yaw aspect system (Zehnder *et al.*, 2002; Fivian *et al.*, 2002) can be used to compensate for time-varying pointing. In addition, accurate absolute knowledge (1 arc min, 1σ) of the roll orientation is required both to coherently interpret the time-modulated light-curves and to accurately place the reconstructed image on the Sun.

Solar Physics **210:** 101–113, 2002.

A number of options were considered for obtaining this roll knowledge. Available non-solar aspect sensors included horizon crossing indicators, star cameras, magnetometers, and differential GPS. Horizon crossing indicators generally have insufficient angular resolution to meet the requirements, as does differential GPS on a spacecraft the size of RHESSI. Model magnetic fields would be required to use a magnetometer as an aspect sensor, and these are neither sufficiently accurate nor stable to meet RHESSI's requirements. In addition having significant cost, power, mass and telemetry implications, most off-the-shelf star cameras are designed for 3-axis stabilized spacecraft and are not well suited to deal with the RHESSI spin rate. Another significant challenge for star sensors is handling the Earth albedo. The sensor will look directly at the sunlit Earth for almost half of rotation, and must come out of saturation in time to measure relatively dim stars.

To meet these requirements, RHESSI has two redundant roll aspect systems: a CCD-based Roll Aspect System (RAS) (Zehnder *et al.*, 2002; Fivian and Zehnder, 2002) and a Photo-Multiplier Tube Roll Aspect System (PMTRAS). The latter was added as a backup system at a late stage of the development of the RHESSI hardware. Both systems are star scanners that view a star field perpendicular to the spin axis. As the spacecraft rotates, the instruments accurately note the times at which bright stars pass through their field of view. With knowledge of the stars' location and confidence in the inertial rotation of the spacecraft, the roll orientation of the spacecraft at any intermediate time can then be interpolated. At the nominal spin rate of 15 rpm, the 1-arc min angular resolution requirement is equivalent to a timing requirement of 0.2 ms.

The PMTRAS was implemented by adapting a low-cost flight-proven star scanner, developed by M. Lampton for rocket payloads, to meet RHESSI's requirements. Both RAS and PMTRAS are operational, but RHESSI imaging to date has been based on the PMTRAS.

The purpose of this paper is to describe the PMTRAS principles of operation, hardware implementation, calibration, performance and software. In Section 2, the hardware is summarized. Pre- and post-launch calibrations are described in Section 3. Performance issues are discussed in Section 4, followed by an outline of the data analysis approach in Section 5.

2. Hardware Description

2.1. Optics

A schematic view of the PMTRAS optics is shown in Figure 1. It consists of a primary 75 mm focal length $f/3$ plano-convex singlet lens, stopped down to 22 mm, that focuses an image of the star field onto a 6.5×0.02 mm slit. Optical distortions due to the use of a singlet, primary lens are not important since only the integrated light distributed along the slit is relevant. A secondary re-imaging

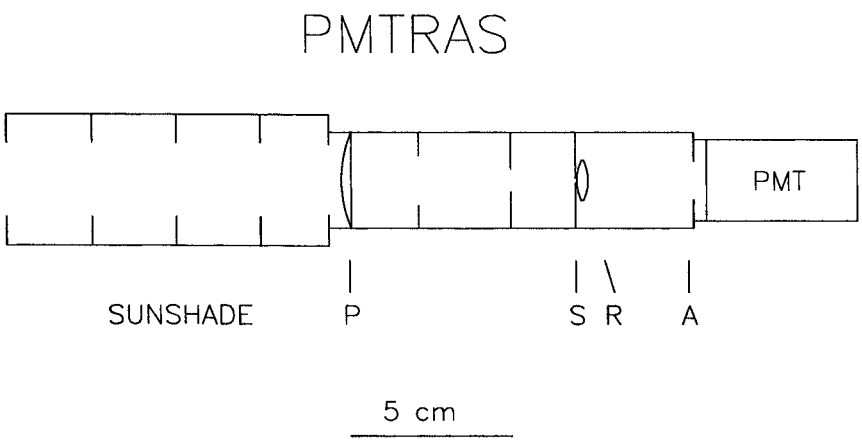

Figure 1. Profile of the PMTRAS optics in the plane orthogonal to the slit, S, showing the primary lens, P, the reimaging lens, R, and PMT aperture, A.

singlet lens with a 25 mm focal length distributes the light passed by the slit over a 12 mm diameter aperture over the face of a 1-inch R1924-01 Hamamatsu photomultiplier tube (PMT) whose bialkali photocathode is nominally sensitive from 300 to 650 nm. The peak system response is at 420 nm. Fused silica lenses were used to provide good ultraviolet transmission and to minimize radiation damage.

The use of a singlet lens results in a focal length that is wavelength dependent but for most star classes provides a nominal 0.07 mm r.m.s. focal spot. Convolving this with the slit width implies a FWHM response of 10 arc min on the sky. This corresponds to a 2 ms FWHM transient signal (*blip*) at 15 rpm. The field of view parallel to the spin axis is 5 deg, centered at a polar angle of 90 deg. A sunshade suppresses illumination by a factor of $> 10^6$ outside an unobstructed 15-deg field of view.

2.2. Electronics

The PMTRAS electronics includes the PMT, along with its bias supply and bleeder chain, a charge sensitive preamp/discriminator, and logic circuitry that accumulates counts and interfaces to the RHESSI Instrument Data Processing Unit (IDPU) (Curtis *et al.*, 2002). Since the PMTRAS was added late in the RHESSI development process, it was constrained to fit with the existing spacecraft and instrument hardware design, while using as much off-the-shelf design and hardware as possible. An existing flight-spare PMT and HV bias supply from the WIND 3D Plasma instrument were found to meet the sensitivity requirements. An Amptek A111 charge-sensitive preamp / discriminator was used to convert the anode charge pulses into logic pulses. These pulses were then passed to a Field Programmable Gate Array (FPGA). This FPGA contained counters and logic to interface the

PMTRAS data to the RHESSI IDPU. The FPGA was mounted on a small daughter board attached directly to the IDPU backplane.

One issue that had to be addressed was that the PMTRAS would face the bright Earth albedo once per rotation during the sunlit portion of the orbit. To speed recovery from this condition, modifications were made to the bleeder chain that distributes high voltage among the subsequent dynodes in the PMT. The photocathode current is sensed, and when it exceeds a set level, the bias to the first dynode of the PMT is shorted out. This greatly reduces the gain of the PMT, avoiding excessive rates at the later dynodes that can cause aging. This also speeds the PMT recovery during transitions from Earth- to space-viewing each spacecraft rotation.

The PMT and its bleeder chain and bias supply were packaged with the PMTRAS optics and attached directly to the side of the IDPU. This provided the desired FOV without affecting spacecraft interfaces.

2.3. Telemetry

The basic data acquired by the PMTRAS consist of digitized output pulses from the PMT. These pulses are summed in counters with *accumulation intervals* of a few milliseconds (programmable by ground command to $\frac{1}{256}$, $\frac{1}{512}$ or $\frac{1}{1024}$ s).

To accommodate this 8 kbps data rate within the instrument diagnostic telemetry allocation of 128 bps, the FPGA looks for the maximum count in a $\frac{1}{4}$ s *readout interval* (also programmable in powers of 2). The telemetry then includes the time of the sample containing the maximum number of counts in the readout interval, the maximum counts in that interval and the counts in the preceding and following intervals. Nominally, the maximum corresponds to the brightest object (star) seen in the readout interval. Since counts from a typical star are divided among 2 or 3 of the recorded accumulation intervals, interpolation to accuracy much better than the 2 ms accumulation time is possible. After compressing the counts to 8 bits, each readout requires 4 bytes. This meets the 128 bps telemetry requirement while providing information on up to 16 stars per rotation.

3. Calibration

3.1. Prelaunch calibration

The key calibration requirement is to determine the direction of maximum response of the PMTRAS optics with respect to the orientation of the imager grids to 1 arc min. It is important to note that errors in this calibration have no effect whatsoever on the morphology of the reconstructed image. Rather, this knowledge serves only to place the image at the correct position angle with respect to Sun center. For a spin axis at Sun center and a limb flare, a 1-arc min roll error corresponds to a 0.3 arc sec image location error.

This calibration was conducted after the PMTRAS was mounted on the spacecraft by noting the amplitude of the PMTRAS response to a blinking diode that was slowly moved in azimuth at two successive different radii (~ 3 and ~ 6 m). Theodolites were used to relate the diode positions at maximum response to tooling balls on the imager hardware, whose positions, in turn, were known with respect to grid orientations to $\ll 1$ arc min. Redundant measurements provided an internal consistency of ± 0.01 deg that met the requirement.

Knowledge of the dead time of the PMT response is necessary for correcting count rates observed for the brightest stars. This was determined by noting the relative count rates as a fixed blinking source was moved radially from the PMTRAS. The measured dead time was 0.9 μs, which enables input count rates up to $\sim 2 \times 10^6$ counts s^{-1} to be corrected.

3.2. Post-launch calibration

Post-launch calibrations permit improvements in both the relative and absolute accuracy of the roll data. The most important of these calibrations is based on observations of the Crab nebula during its annual passage within 1.5 deg of the Sun on 15 June. This is sufficiently close that while nominally observing the Sun, the Crab passes within the imaging field of view. When analysis of these data is complete, the reconstructed location of the Crab pulsar will confirm (or correct) our knowledge of the orientation of the roll aspect system with respect to the grids to a level of accuracy of ~ 0.1 arc min, well in excess of the solar requirement.

Statistical analyses of the observed star field can be used to calibrate some instrument parameters. For example, an initial analysis of which stars were detected (or not) was used to confirm the polar alignment and field of view of the slit to ± 0.2 deg. In the future, the precision of the roll solution will benefit from self-calibration of the orientation of the slit, which can be inferred from systematic phase shifts from stars observed at different polar angles.

Statistical analysis of the distribution of counts for each star can be used to infer the pulse shape and width, since the instant of maximum count rate should be randomly distributed within integration intervals. Preliminary analysis has yielded an average pulse width of about 2.6 ms, slightly higher than expected for a rotation rate of 14.5 rpm. The observed distributions also suggest that some star classes generate an asymmetrical pulse shape.

4. Performance

One of the advantages of using a PMT in this application is that signal-to-noise is dominated by the integrated background star field rather than electronic noise. Since reaching its nominal spin period of 15 rpm on 27 Februray 2002, normal operation of the PMTRAS has used the 2 ms integration time option. The number

of counts due to the integrated background star field varies widely depending on proximity to the galactic plane and on orbital phase. In a 2 ms interval, typical values range from a few tens to a few hundreds of counts. This dominates the PMT noise, which is estimated to be about 2 counts. Prelaunch expectations for counts from magnitude 4 stars ranged from ~ 30 to ~ 150 counts in a 2 ms interval, depending on spectral class (M0 to B0). In-flight sensitivity has proved to be consistent with this. No significant degradation in PMTRAS sensitivity has been noted in the first few months of operation.

For any given orbit, the visible star field represents a 5-deg band that intersects the ecliptic poles. During the year, this band rotates about the poles so that a substantially different star field is sampled every few days. As a result, the number of observed stars varies significantly both with time of year as well as with orbital phase. Typically several tens of valid blips are detected per minute, representing from 1 to ~ 10 different stars.

PMTRAS measurements of spin period for typical orbits are shown in Figure 2. Although ideally RHESSI would spin with a constant angular velocity, the spin period is in fact not uniform. Within each orbit there is an asymmetrical cyclic variation in the spin period of 2 ms peak-to-peak. This is associated with thermal expansion and contraction of the solar panels due to the day/night cycle and with power generation that further heats the panels during the first part of the sunlit portion of each orbit. (The solar panels expand at higher temperatures, increasing their moment of inertia and so lengthening the spin period.) The temporal profile is generally smooth, except for sharp (~ 30 s) 'snaps' that occur as the spacecraft enters and leaves sunlight. In addition, there is a systematic ~ 0.25 ms increase in rotation period each orbit, which is probably due to secondary effects of the torque-rod-based aspect control system.

5. Data Analysis

5.1. Data analysis steps

As previously discussed, the raw PMTRAS data consist of 4 potential star 'blips' per second, each of which defines the time and the values of 3 successive 2-ms accumulations of counts. The data analysis objective is to convert these data into knowledge of absolute roll angle as a function of time.

Since many of the blips are due to causes other than stars, the first step is to filter the 4-Hz dataset. Albedo response is suppressed by rejecting blips if the *minimum* of the 3 counts exceeds 1000 counts. A diagnostic check of PMT operation flags blips if the *maximum* count is less than 2. To suppress cases where the remaining albedo or background star field still dominates, a requirement is imposed that the difference between the minimum and maximum counts among the 3 samples be statistically significant at the 4.5σ level. After such filtering, most of the remaining

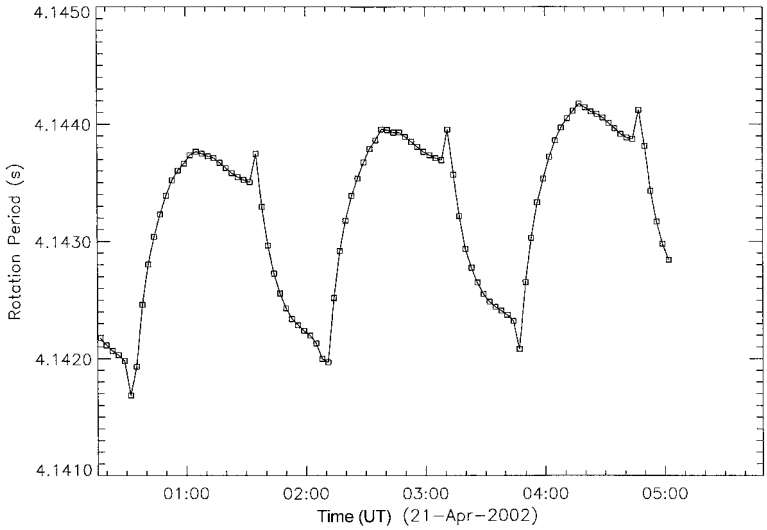

Figure 2. Preliminary estimates of rotation period for a typical 3-orbit interval that in this case includes RHESSI's first X-class flare on 21 April 2002. The six sharp changes occur at successive entries into sunlight and into eclipse.

valid blips represent well-observed stars although a few have a terrestrial origin ('city lights').

The next step is to determine a more precise occurrence time of each valid blip within its identified 2-ms integration interval. To that end, a timing parameter, R, is defined as

$$R = \frac{(\mathrm{C2} - \mathrm{C0})}{(\mathrm{C1} - \min(\mathrm{C2}, \mathrm{C0}))} ,$$

where C0, C1, C2 are the counts observed in the 3 successive integration intervals (C1 > C0, C2). R has the property that it is independent of background and source intensity, and for any given pulse profile will increase monotonically as the occurrence time of the blip advances through the 2-ms accumulation interval. The complete set of valid blips are time-ordered on the basis of R and assigned equally spaced time slots within the 2-ms interval slots on the basis of this ordering. (The rationale is that blip times should occur randomly within a 2-ms interval.) For a dataset containing a large number of blips, the interpolated time has an accuracy that is dominated by counting statistics and does not depend on knowledge of the blip time profile. For typical analyses, interpolated blip times are good to ~ 0.1 ms.

A set of preliminary estimates of rotation period are obtained every 3 min by identifying recurring time differences (and integral multiples thereof) among the blips. This technique exploits the high timing accuracy of the blips and is robust in the face of missing blips, irregular occurrence of multiple blips per rotation, and the presence of blips of non-stellar origin. Figure 2 shows a typical sequence of such periods.

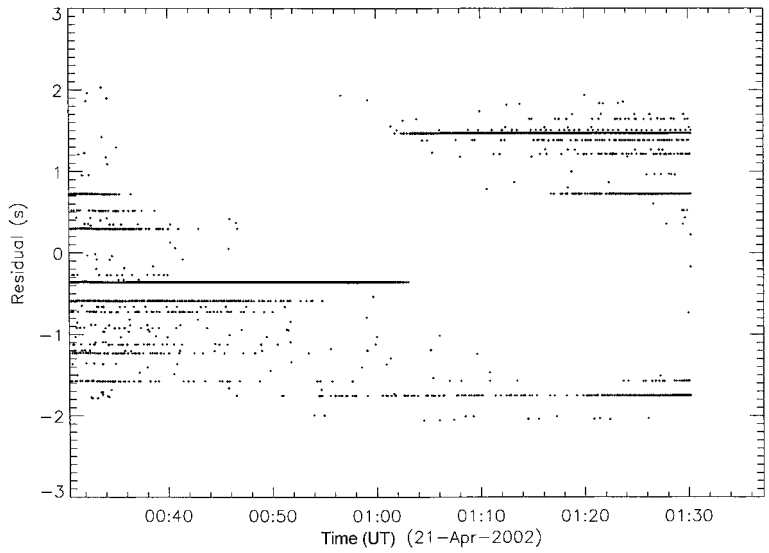

Figure 3. Preliminary timing residuals for the first orbit shown in Figure 2. Each point represents an observed 'blip'. The timing residual corresponds to the difference between the observed time of the blip and the time at which the spacecraft had a fixed (but arbitrary) roll orientation as determined from the periods in Figure 2. Each star has the same timing residual on successive rotations and so appears as a horizontal line. The diagonal blank area corresponds to intervals in each rotation when the PMTRAS was viewing the Earth.

The sequence of average preliminary rotational periods determines a set of reference times at which the spacecraft has the same position angle. The observed blip times are then expressed as a set of a time residuals, relative to the closest reference time (Figure 3).

The timing residuals for each blip are converted to rotational phases (still with an arbitrary zero) and are associated with their intensity as shown in Figure 4. In principle, at this stage all blips associated with a given star should have the same intensity and relative phase. In practice, as Figure 4 suggests, the phase scatter is much better than that of the intensity, which typically varies by $\sim \times 2$ for a given star. (The poor photometry arises because inaccurate background subtraction results in a dependence of apparent intensity on the occurrence time of a blip within the accumulation interval.) The relative phases (and to a lesser extent their intensities) are used to identify up to ~ 10 groups of blips, each associated with individual stars whose identities are unknown at this stage. Averaging within each 'blip group' then yields a best estimate of the relative phase for each blip group.

To associate the blip groups with specific stars, a database, derived from the Yale bright star catalog, is used to convert precessed star positions to a set of potentially detectable stars for a given date and time. Such a subset typically contains ~ 100 stars whose positions are expressed in terms of position angle. To minimize potential identification errors, stars with closely spaced position angles are discarded

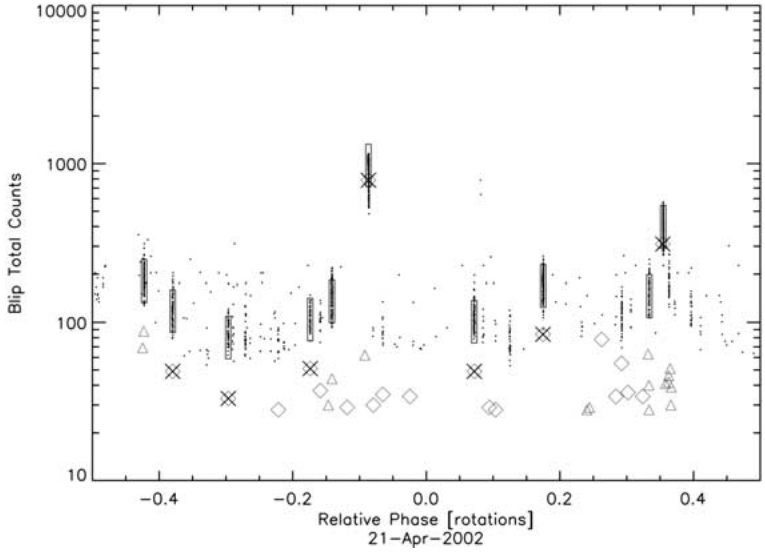

Figure 4. Intensity/phase correlation for the same observed 'blips' shown in Figure 3. The relative phase is the ratio of the timing residual to the rotation period. The tall *rectangles* identify groups of blips that were associated with a specific star. The *diamonds* represent stars that could potentially be observed, plotted as predicted star intensity/phase in the same units and same relative phase as the observed blips. The 7 '×'s indicate stars that were identified with the blip group that appears above them. *Triangles* represent potential stars that were not considered because of proximity in position angle to other stars.

from this list unless one is much brighter than the other, in which case the stronger one is retained.

At this stage, we have M (~ 10) observed 'blip groups' with accurate *relative* rotational phases but whose absolute position angles are unknown. The next objective is to associate these with specific stars (with known position angles) selected from the N (~ 100) element subset of bright stars. Given the $\sim N^M$ possibilities, this cannot be done on a trial-and-error basis. Instead, the more tractable $M \times N$ possible cases of association of a single star are considered. In each case the position angles of all 'blip groups' are shifted on the basis of the trial association and position angle differences between the remaining 'blip groups' and nearest star are evaluated. The best association is based on the number and proximity of matches between the two groups. This works very quickly and reliably, provided accurate relative observed blip-group phases are available. Typically, star associations for about 2 to 6 blip groups are obtained.

By this point, all blips within 'associated blip groups' have been associated with specific stars. All other blips and all preliminary estimates of rotation period are discarded. The associated blips now define a sequence of monotonically increasing position angles as a function of time. After rejection of a few outliers and converting to a table of spacecraft Y-axis orientations (clockwise relative to solar north)

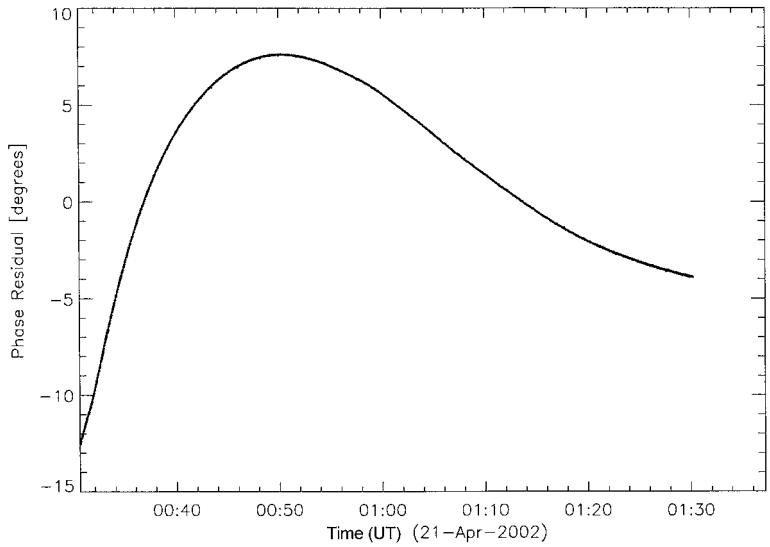

Figure 5. The final roll solution, plotted as a phase residual relative to a best-fit fixed period of 4.143114 s. The data consist of all star-associated blips in Figure 4.

as a function of time, this becomes the output of the PMTRAS. Figure 5 shows a typical plot of the results, expressed as a phase relative to a best-fit fixed period. The magnitude of the phase variations demonstrates the need to accommodate the non-uniform rotation period for integrations of a few minutes or more. The single-valued nature of the curve, which is based on multiple stars, provides strong confirmation of the correct star association. Figure 6 shows a subset of this data over a more limited time to illustrate typical scatter for individual blips. At any time, the scatter is ~ 0.03 deg peak-to-peak. Even without averaging, these data can be linearly interpolated to yield position angle with an accuracy of < 1 arc min r.m.s.

Note that for this level of accuracy, and for solar pointing accurate to 0.2 deg, the PMTRAS solution does not require any correction based on the pitch and yaw pointing of the spacecraft to meet the accuracy requirements for solar imaging.

5.2. Data analysis issues

There are a number of assumptions that must be fulfilled to make the foregoing sequence of analysis steps work in practice. First, several different stars must be observed during the analysis interval. Second, appropriate thresholds must be set so that there are not too many potential stars with which to evaluate trial associations. Third, during the analysis interval there must be no significant PMTRAS data gaps or extended periods of no viable star observations. Satisfaction of this condition is necessary so that coherent initial phases can be derived to support star identification. These conditions can be satisfied by appropriate selection of PMTRAS

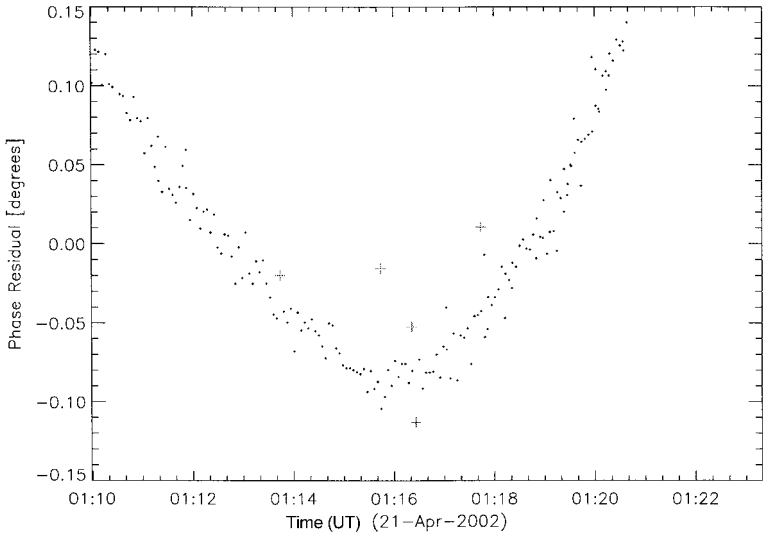

Figure 6. An expanded view over a 10-min interval in Figure 5, shown relative to a locally-fit fixed period of 4.143686 s. The peak-to-peak scatter of individual measurements at any specific time is ~ 0.03 deg.

analysis parameters. Although this can almost always be done manually, automated selection of such parameters sometimes results in one or more of these conditions not being satisfied.

The fundamental reason for the failure of automated selection of PMTRAS analysis parameters is rooted in the character of the RHESSI analysis software. In order to retain the flexibility that RHESSI provides for users to select analysis parameters (such as image-, time- and energy- resolution and range), most users analyzing RHESSI data start from level-0 data and perform calibration tasks on-the-fly. This approach works well for X-ray analyses over a wide range of time intervals. However, the optimum PMTRAS analysis intervals are based on other considerations. For example, sometimes it is desirable to span a substantial portion of an orbit to support star identification, but at other times this is undesirable, since an extended interval may incorporate an unbridgeable data gap. Failure to select appropriate parameters can result in unnecessary gaps in the PMTRAS solution or, more usually, in false star associations. A roll solution with false star association will still provide images with the correct morphology, but their placement in position angle about Sun center is arbitrary.

While manual PMTRAS analysis with appropriate parameters is certainly a viable solution to this dilemma, this approach would be incompatible with our goal of making image reconstruction as transparent as possible to the user.

A second set of problems is associated with the presence of data gaps in the PMTRAS dataset. These arise because the PMTRAS shares a small (1000 packet) data buffer with other diagnostic information. In circumstances where (intention-

ally or inadvertently) the data buffer becomes full, no PMTRAS data is stored until the next ground contact. In the first six months of the mission, such gaps average about 4% of the total mission time and typically last many minutes. In some cases, interpolation can be used to achieve a useful solution.

5.3. FUTURE DEVELOPMENTS

The highest priority future development associated with PMTRAS roll aspect solution is the elimination of problems associated with automated selection of analysis parameters. Although it means establishment of a secondary database, a mission-long roll solution will be generated that will provide a roll solution applicable to any user-specified time interval. Such an approach is also well suited to the expected eventual integration of RAS and PMTRAS analysis outputs and to non-solar analyses over extended time intervals. This database will also incorporate the obvious improvement of averaging the PMTRAS output on a ~ 1 min timescale. This should reduce the current ~ 1 arc min scatter by an order of magnitude.

Additional improvements in the roll calibration will result from analysis of the Crab pulsar observations described above and from further analysis of the in-flight self-calibrations.

6. Discussion

The RAS and PMTRAS systems provide redundant information on RHESSI roll aspect. They are complementary in several respects: the PMTRAS sensitivity is limited by the background star field whereas the RAS sensitivity is limited by electronic noise; the RAS and PMTRAS sensitivities peak in the red and blue respectively; the RAS has lower sensitivity but a wider (30 deg) field of view and views a different field; they employ different techniques for albedo suppression and recovery. Thus they are well suited to providing redundant roll information.

Although the PMTRAS was a late and inexpensive addition to the RHESSI mission, it has proved successful in terms of providing roll aspect with the required accuracy and reliability. The primary difficulty has been due to the application of flexible, user-specified analysis parameters to a subsystem whose data analysis is better matched to the traditional approach that provides users with calibrated output. This will be addressed in the near future with the generation and distribution of a roll-solution database.

Acknowledgements

We thank Paul Turin of SSL who was responsible for the mechanical design and assembly of the PMTRAS. We are also grateful to Dave Clark of GSFC for his

exemplary work (as always) in the optical calibration. This work was supported by NASA grant NAS5-98033-05/03.

References

Curtis, D. W. *et al.*: 2002, *Solar Phys.*, this volume.
Fivian, M., Hemeck, R., Mchedlishvili, and Zehnder, A.: 2002, *Solar Phys.*, this volume.
Hurford, G. J. *et al.*: 2002, *Solar Phys.*, this volume.
Lin, R. P. *et al.*: 2002, *Solar Phys.*, this volume.
Schwartz, R. A., Csillaghy, A., Tolbert, A. K., Hurford, G. J., McTiernan, J., and Zarro, D.: 2002, *Solar Phys.*, this volume.
Zehnder, A. *et al.*: 2002, *SPIE Proc.* **4853**, in press.